Ionics (2009) 15:743–747
DOI 10.1007/s11581-009-0340-6

SHORT COMMUNICATION

Electro-oxidation of ethanol using PtRuBi/C electrocatalyst prepared by borohydride reduction

M. Brandalise · R. W. R. Verjulio-Silva · M. M. Tusi · O. V. Correa · L. A. Farias · M. Linardi · E. V. Spinacé · A. Oliveira Neto

Received: 29 January 2009 / Revised: 26 February 2009 / Accepted: 26 March 2009 / Published online: 8 April 2009

Abstract Pt/C, PtRu/C, PtBi/C, and PtRuBi/C electrocatalysts (20 wt.% metal loading) were prepared by borohydride reduction using $H_2PtCl_6 \cdot 6H_2O$, $RuCl_3 \cdot xH_2O$, and $Bi(NO_3)_3 \cdot 5H_2O$ as metal sources and Vulcan XC 72 as support. The electrocatalysts were characterized by energy-dispersive X-ray analysis, X-ray diffraction, and thermogravimetric analysis. The electro-oxidation of ethanol was studied in sulfuric acid solution by cyclic voltammetry and chronoamperometry. The electrochemical studies showed that PtRuBi/C (50:40:10) electrocatalyst has superior performance for ethanol electro-oxidation at room temperature compared to the other electrocatalysts. Preliminary tests at 100 °C on a single direct ethanol fuel cell also confirm the results obtained by electrochemical techniques.

Keywords PtRuBi/C electrocatalyst · Borohydride reduction · Ethanol oxidation · Direct ethanol fuel cell

Introduction

The use of hydrogen in fuel cell technology has some limitations due to problems associated with production, purification, distribution, and principally storage. Then, the use of liquid fuels is of great interest, and methanol has been considered the most promising fuel because it is more efficiently oxidized than other alcohols. On the other hand, slow anode kinetics has been observed and it is considered a toxic product [1–4]. Thus, ethanol has been considered as an alternative fuel because it can be produced in large quantities from agricultural products and it is the major renewable biofuel from the fermentation of biomass. However, its complete oxidation to CO_2 is more difficult than that of methanol due to the difficulty in C—C bond breaking and to the formation of CO intermediates that poison the platinum anode catalysts. In this context, more active electrocatalysts are essential to enhance the ethanol electro-oxidation [1–4].

Carbon-supported platinum is commonly used as anode catalyst in low temperature fuel cells; however, pure Pt is not an efficient anodic catalyst for the direct ethanol fuel cell. Platinum itself is known to be rapidly poisoned on its surface by strongly adsorbed species coming from the dissociative adsorption of ethanol. Efforts to mitigate the poisoning of Pt have been concentrated on the addition of co-catalysts to platinum. In recent years, it was found that certain metal oxides such as RuO_2 can enhance the catalytic activity for ethanol and methanol electro-oxidation through synergetic interaction with Pt [5, 6]. The Pt sites act as adsorption and dehydrogenation centers for ethanol, while the Ru sites provide oxygen-containing species at lower potentials than those on a pure Pt surface. The PtRu/C electrocatalysts have some attractive properties, but they still exhibit significant overpotentials for the oxidation of small organic molecules; consequently, it is necessary to develop new and more efficient PtRu electrocatalysts [5, 6]. It has been described that the addition of a third element to PtRu/C electrocatalyst could increase its activity for ethanol oxidation. The role of the third component is to facilitate the CO oxidation and/or to reduce the CO adsorption on Pt sites [7–12].

Recently, Disalvo [13–15] reported the use of intermetallic PtBi as alternative materials for fuel cell applications. In these studies, PtBi showed some immunity to CO

M. Brandalise · R. W. R. Verjulio-Silva · M. M. Tusi · O. V. Correa · L. A. Farias · M. Linardi · E. V. Spinacé · A. Oliveira Neto (✉)
Instituto de Pesquisas Energéticas e Nucleares, CNEN/SP, São Paulo, SP 05508-000, Brazil
e-mail: aolivei@ipen.br

poisoning; this behavior is a key characteristic for a direct alcohol fuel cell. The catalytic action of Bi was interpreted in terms of electronic effect and enhanced adsorption of OH species on adjacent Pt sites. The use of PtBi/C for formic acid oxidation was also described [16–18]; its enhanced catalytic activity compared to Pt/C was related to electronic effects, which enhanced the affinity of PtBi for formic acid adsorption, and to the formation of surface oxides at low potentials, as well as to geometric effects reducing the affinity for CO poisoning.

In this aspect, PtRuBi/C electrocatalyst was prepared by borohydride reduction and tested for ethanol electro-oxidation.

Experimental

Pt/C, PtBi/C, PtRu/C, and PtRuBi/C electrocatalysts (20 wt.% metal loading) were prepared in a single step using $H_2PtCl_6{\cdot}6H_2O$, $RuCl_3{\cdot}xH_2O$, and $Bi(NO_3)_3{\cdot}5H_2O$ as metal sources, sodium borohydride as reducing agent, and carbon Vulcan XC72 as support. The metal sources were dissolved in a mixture of water/2-propanol (50/50, *v*/*v*) and the carbon support was dispersed in the solution. A solution of sodium borohydride was added drop by drop and the final mixture was kept under stirring for 30 min. Finally, the mixture was filtered and the solid was washed with water and dried at 70 °C for 2 h.

X-ray diffraction (XRD) analyses were performed using a Rigaku diffractometer model Miniflex II using Cu Kα radiation source (λ=0.15406 nm). The diffractograms were recorded from 2θ=20° to 90° with a step size of 0.05° and a scan time of 2 s per step.

The atomic ratios were obtained by energy-dispersive X-ray (EDX) analysis using a scanning electron microscope Phillips XL30 working at 20 kV and equipped with EDAX DX4 microanalyzer.

The metal loadings (wt.%) were determined by thermogravimetric analysis (TGA) using a Shimadzu TGA-50 instrument and platinum pans. Heating rate of 5 °C min^{-1} was employed under dry oxygen (30 mL min^{-1}) [19].

Electrochemical studies were carried out using the thin porous coating technique [20]. An amount of 20 mg of the electrocatalysts was added to a solution of 50 mL of water containing three drops of 6% polytetrafluoroethylene (PTFE) suspension. The mixture was treated in an ultrasound bath for 10 min and transferred to the cavity of the working electrode. The working electrodes have a geometric area of 0.4 cm^2 with a depth of 0.3 mm. The reference electrode was a RHE and the counter electrode was a platinized Pt plate.

In cyclic voltammetry and chronoamperometry experiments, the current values (*I*) were expressed in amperes and were normalized per gram of platinum (A g_{Pt}^{-1}) [11, 20]. The quantity of platinum was calculated considering the mass of the electrocatalyst present in the working electrode multiplied by its percentage of platinum. Cyclic voltammetry and chronoamperometry experiments were performed at 25 °C with 1.0 mol L^{-1} of ethanol in 0.5 mol L^{-1} H_2SO_4 solutions saturated with N_2 using a Microquímica (model MQPG01, Brazil) potentiostat/galvanostat.

The membrane electrode assemblies (MEA) were prepared by hot pressing a pretreated Nafion® 117 membrane placed between either a Pt/C, PtBi/C, PtRu/C, or PtRuBi/C anode (1 mg Pt cm^2 catalyst loading) and a 20 wt.% Pt/C E-TEK cathode (1 mg Pt cm^2 catalyst loading) at 125 °C for 2 min under a pressure of 225 kgf cm^2. The direct ethanol fuel cell performances were determined in a single cell with an area of 5 cm^2. The temperature was set to 100 °C for the fuel cell and 80 °C for the oxygen humidifier. The fuel was 2 mol L^{-1} ethanol solution delivered at approximately 2 mL min^{-1} and the oxygen flow was regulated at 500 mL min^{-1} and pressure of 2 bar. Polarization curves were obtained by using a TDI RBL 488 electronic load.

Results and discussion

The Pt:Bi, Pt:Ru, and Pt:Ru:Bi atomic ratios of the obtained electrocatalysts were similar to the nominal atomic ratios and the mean crystallite sizes determined using Scherrer equation [11, 20] were in the range of 3–4 nm, except for PtBi/C electrocatalyst that was 7 nm (Table 1). The metal loading (wt.%), determined by TGA analysis [19], showed the presence of 17–20 wt.% of metals for the different electrocatalysts prepared (Table 1 and Fig. 1).

The X-ray diffractograms of the electrocatalysts were shown in Fig. 2. Pt/C, PtRu/C, PtBi/C, and PtRuBi/C electrocatalysts showed a broad peak at about 2θ=25° that

Table 1 Atomic ratios, metal loading, and crystallite size of the Pt/C, PtRu/C, PtBi/C, and PtRuBi/C electrocatalysts

Electrocatalyst	Nominal atomic ratio	Atomic ratio—EDX	Metal loading (wt.%)	Crystallite size (nm)
Pt/C	–	–	18	4
PtBi/C	50:50	48:52	19	7
PtRu/C	50:50	57:43	17	3
PtRuBi/C	50:40:10	42:43:15	20	3

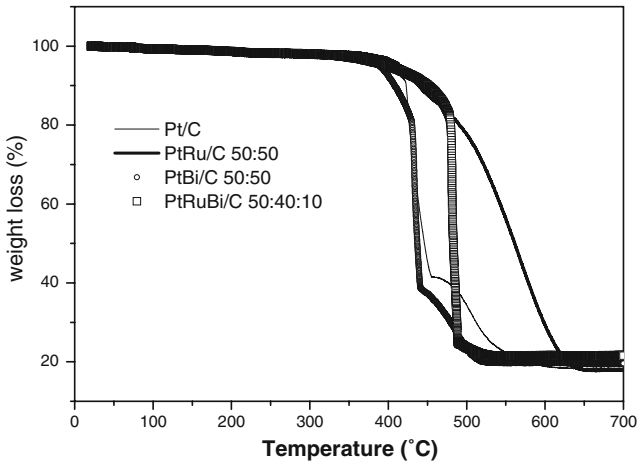

Fig. 1 Thermogravimetric analysis of Pt/C, PtRu/C, PtBi/C, and PtRuBi/C electrocatalysts after thermal treatment under dry oxygen (30 mL min^{-1}) and heating rate of 5 °C min^{-1}

was associated with the carbon support and five diffraction peaks at about 2θ=40°, 47°, 67°, 82°, and 87° characteristic of the face-centered cubic (fcc) structure of platinum and platinum alloys. The diffractogram of PtRu/C electrocatalyst showed the five diffraction peaks of fcc phase shifted to higher angles with respect to those of Pt/C electrocatalyst, indicating a lattice contraction and alloy formation. No peaks corresponding to a metallic ruthenium, materials rich in ruthenium with a hexagonal structure, or the ruthenium oxide phase were observed [11]. For PtBi/C electrocatalyst, the five diffraction peaks of fcc phase are shifted to smaller angles indicating a lattice expansion and suggesting that bismuth atoms were incorporated into fcc lattice. In this case, peaks were also observed at about 2θ= 23°, 29°, 33°, 53°, and 57° that could be attributed to Bi_2O_3 phases [21–28]. The diffractogram of PtRuBi/C electrocatalyst showed the five diffraction peaks of fcc phase shifted to higher angles, but the shift was small compared to the one observed for PtRu/C electrocatalyst; and the diffraction peaks attributed to Bi_2O_3 phases were also observed in the diffractogram.

The cyclic voltammograms (CV) of Pt/C, PtBi/C, PtRu/C, and PtRuBi/C electrocatalysts in the absence of ethanol are shown in Fig. 3. The CV of PtBi/C, PtRu/C, and PtRuBi/C electrocatalysts do not have a well-defined hydrogen adsorption–desorption region (0.05–0.4 V) in comparison with Pt/C electrocatalyst and an increase in the current values in the double layer (0.4–0.8 V) were also observed, which may be attributed to the formation of bismuth and/or ruthenium oxide species. Analysis of the cathodic scan also showed an increase in the currents in the double layer that could be associated with the reduction of oxide species in the catalyst. PtBi/C also showed that the hydrogen adsorption region is greatly reduced by the presence of Bi in comparison with Pt/C, PtRu/C, and PtRuBi/C. Notably, the presence of bismuth in PtBi leads to the formation of two peaks located close to 0.63 and 0.78 V [18].

The CV of Pt/C, PtBi/C, PtRu/C, and PtRuBi/C electrocatalysts in 0.5 mol L^{-1} H_2SO_4 and 1.0 mol L^{-1} ethanol are shown in Fig. 4. The cyclic voltammetry responses were normalized per gram of platinum, considering that ethanol adsorption and dehydrogenation occur only on platinum sites at ambient temperature [11, 20]. For all electrocatalysts, the current values in the hydrogen region (0.05–0.4 V) decrease in the presence of ethanol compared to the CVs in the absence of ethanol, most likely due to the adsorption of ethanol and intermediates on the nanoparticle surface, being able to cause the partial deactivation of the electrocatalysts. For Pt/C and PtBi/C electrocatalysts, ethanol electro-oxidation started only at approximately 0.5 V while for PtRu/C and PtRuBi/C electrocatalysts the onset potential was shifted negatively by about 250 mV. In

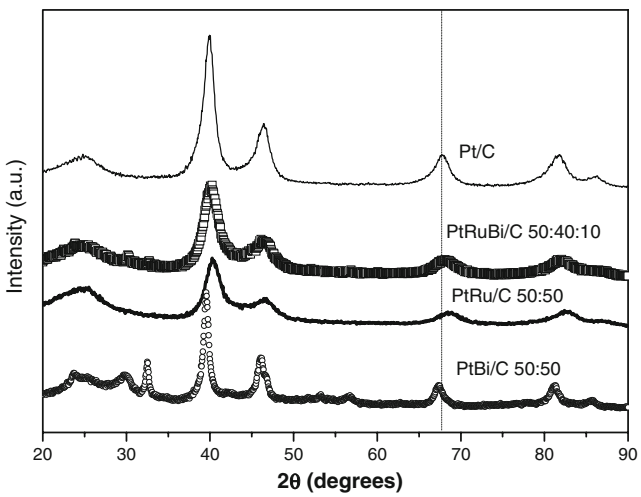

Fig. 2 X-ray diffractograms of Pt/C, PtRu/C, PtBi/C, and PtRuBi/C electrocatalysts

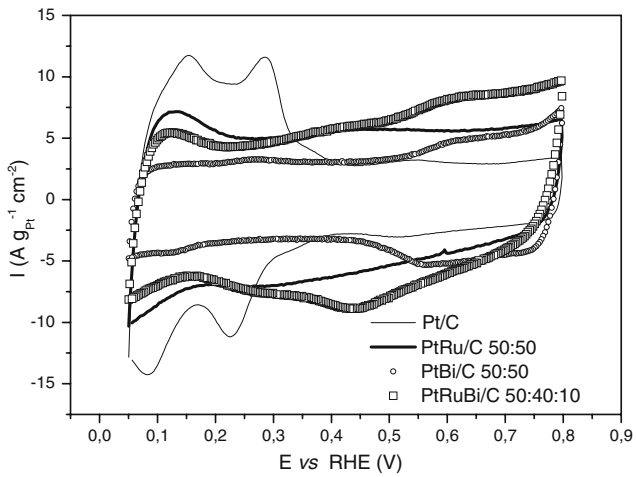

Fig. 3 Cyclic voltammograms of Pt/C, PtRu/C, PtBi/C, and PtRuBi/C electrocatalysts in 0.5 mol L^{-1} H_2SO_4 with a sweep rate of 10 mV s^{-1}

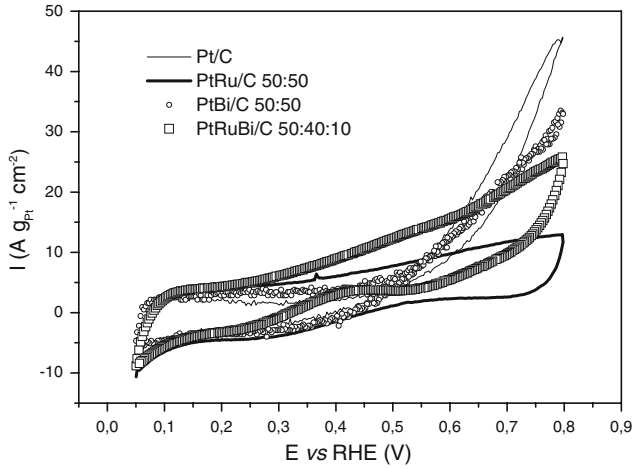

Fig. 4 Cyclic voltammograms of Pt/C, PtRu/C, PtBi/C, and PtRuBi/C electrocatalysts in 0.5 mol L^{-1} H_2SO_4 and 1.0 mol L^{-1} of ethanol with a sweep rate of 10 mV s^{-1}

the potential range of interest for direct ethanol fuel cell (0.2–0.6 V), the current values of PtRu/C and PtRuBi/C electrocatalysts were higher than that of Pt/C and PtBi/C electrocatalysts with PtRuBi/C electrocatalyst showing the best performance for ethanol oxidation.

The chronoamperometry experiments were carried out to examine the electrochemical stability of the electrocatalysts (Fig. 5). The results were obtained in 0.5 mol L^{-1} H_2SO_4 and 1.0 mol L^{-1} C_2H_5OH at an anodic potential of 0.5 V versus RHE. In all chronoamperometric curves, there is a sharp initial current drop in the first 2 min and then the current values practically remain constant until 30 min. The final current values after holding the cell potential at 0.5 V versus RHE for 30 min were the following: PtRuBi/C> PtRu/C>PtBi/C>Pt/C. Oana [29] described that the CO adsorption is drastically reduced on PtBi surfaces with

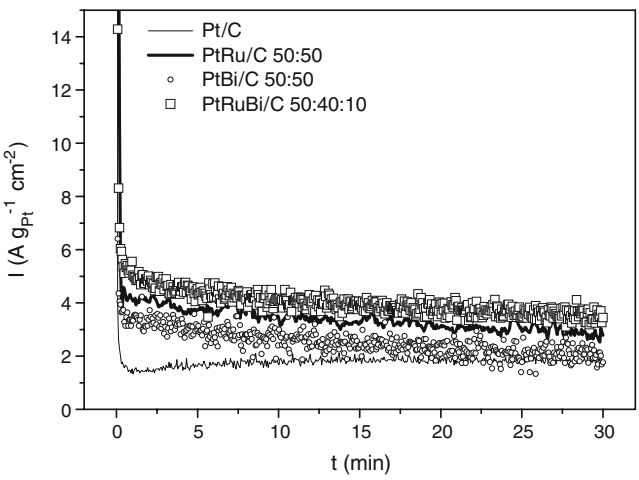

Fig. 5 Current–time curves at 0.5 V in 1 mol L^{-1} ethanol solution in 0.5 mol L^{-1} H_2SO_4 for Pt/C, PtRu/C, PtBi/C, and PtRuBi/C electrocatalysts

respect to bulk of Pt. The XRD measurements of PtRuBi/C electrocatalyst suggest that the Bi atoms were found in the form of alloy and oxides. In this manner, the increase of performance for ethanol oxidation could be related to the reduction of CO adsorption on Pt sites and/or to provide oxygenated species at lower potentials for oxidative removal of adsorbed CO (bifunctional mechanism).

The performances of single cell and the power density of Pt/C, PtBi/C, PtRu/C, and PtRuBi/C as anode catalysts are shown in Fig. 6. The open circuit voltage of the fuel cell containing PtRu/C electrocatalyst was 0.65 V, while that adding Bi to PtRu/C, the corresponding value increases to 0.71 V. Demarconnay [18] also showed that the addition of bismuth to platinum catalysts leads to an increase in the open circuit voltage from 0.66 to 0.83 V in the direct ethylene glycol fuel cell. The maximum power density of PtRuBi/C electrocatalyst (25 mW cm^{-2}) was greater than that of PtRu/C electrocatalyst (20 mW cm^{-2}). Thus, as observed by electrochemical techniques, the use of PtRuBi/C electrocatalyst also increased cell performance.

Conclusion

The borohydride reduction showed to be an effective method for producing active PtRuBi/C electrocatalyst for ethanol oxidation. The X-ray measurements of PtBi/C and PtRuBi/C electrocatalysts suggest that the Bi atoms were found in the form of alloy and oxides. The electrochemical experiments showed that PtRuBi/C electrocatalyst was more active than PtRu/C and PtBi/C electrocatalysts for ethanol oxidation at room temperature. Preliminary tests at

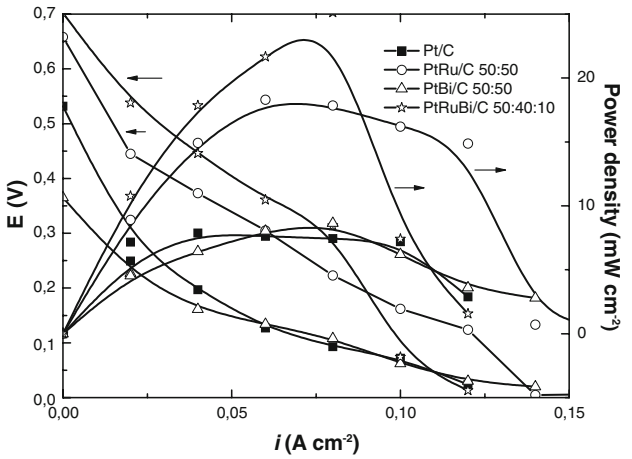

Fig. 6 *I–V* curves of a 5 cm^2 DEFC (←) and the power density (→) at 100 °C using Pt/C, PtRu/C, PtBi/C, and PtRuBi/C electrocatalyst anodes (1 mg Pt cm^2 catalyst loading) and Pt/C E-TEK electrocatalysts cathode (1 mg Pt cm^2 catalyst loading, 20 wt.% catalyst on carbon), Nafion® 117 membrane, ethanol (2.0 mol L^{-1}), oxygen pressure (2 bar)

100 °C on a single DEFC also confirm these results. Further work is now necessary to investigate the PtRuBi/C electrocatalyst surface by different techniques and to elucidate the mechanism of ethanol electro-oxidation.

Acknowledgments The authors thank FINEP-ProH_2, CNPq, and FAPESP for financial support.

References

1. Wendt H, Gotz M, Linardi M (2000) Química Nova 23:538
2. Spinacé EV, Neto AO, Franco EG, Linardi M, Gonzalez ER (2004) Química Nova 27:648
3. Wendt H, Spinacé EV, Neto AO, Linardi M (2005) Química Nova 28:1066
4. Lamy C, Lima A, Lerhum V, Delime F, Coutanceau C, Léger JM (2002) J Power Sourc 105:283
5. Liu H, Song C, Zhang L, Zhang J, Wang H, Wilkinson DP (2006) J Power Sourc 155:95
6. Lux KW, Cairns EJ (2006) J Electrochem Soc 153:A1132
7. Zhou W, Zhou Z, Song S, Li W, Sun G, Tsiakaras P, Xin Q (2003) Appl Catal B 46:273
8. Zhou W, Li W, Song S, Zhou Z, Jang L, Sun G, Xin Q, Poulianitis K, Kontou S, Tsiakaras P (2004) J Power Sourc 131:217
9. Tanaka S, Umeda M, Ojima H, Usui Y, Kimura O, Uchida I (2005) J Power Sourc 152:34
10. Wang Z, Yin G, Zhang J, Sun Y, Shi P (2006) Electrochim Acta 51:5691
11. Oliveira Neto A, Dias RR, Tusi MM, Linardi M, Spinace EV (2007) J Power Sourc 166:87
12. Rousseau S, Coutanceau C, Lamy C, Leger JM (2006) J Power Sourc 158:18
13. Casado-Rivera E, Gal Z, Angelo ACD, Lind C, DiSalvo FJ, Abruna HD (2003) ChemPhysChem 4:193
14. Casado-Rivera E, Volpe DJ, Alden L, Lind C, Angelo ACD, DiSalvo FJ, Abruna HD (2004) J Am Chem Soc 126:4043
15. Volpe DJ, Casado-Rivera E, Alden L, Lind C, Hagerdon K, DiSalvo FJ, Abruna HD (2004) J Electrochem Soc 151:A971
16. Byung-Jun K, Kihyun K, Choong KR, Jonghee H, Tae-Hoon L (2008) Electrochim Acta 53:7744
17. Tripkovic AV, Stevanovic RM, Socha R, Kowal A (2006) Electrochem Comm 8:1492
18. Demarconnay L, Brimaud S, Coutanceau C, Leger JM (2007) J Electroanal Chem 601:169
19. Baturina OA, Aubuchon SR, Wynne KJ (2006) Chem Mater 18:1498
20. Spinace EV, Linardi M, Oliveira Neto A (2005) Electrochem Comm 7:365
21. Roychowdhry C, Matsumoto F, Zeldovich VB, Warren SC, Mutolo PF, Ballesteros M, Wiesner U, Abruna HD, Disalvo FJ (2006) Chem Mater 18:3365
22. Roychowdhury C, Matsumoto F, Mutolo PF, Abruna HD, DiSalvo FJ (2005) Chem Mater 17:5871
23. Fan HT, Pan SS, Teng XM, Ye C, Li GH, Zhang LD (2006) Thin Solid Films 513:142
24. Li W (2006) Mater Chem Phys 99:174
25. Xiong Y, Wu M, Ye J, Chen Q (2008) Mater Lett 62:1165
26. Wang L, Cui ZL, Zhang ZK (2007) Surf Coat Technol 201:5330
27. Laurenta K, Wang GY, Tusseau-Nenez S, Leprince-Wang Y (2008) Solid State Ionics 178:1735
28. Kim HW (2008) Thin Solid Films 516:3665
29. Oana M, Hoffmann R, Abruna HD, DiSalvo FJ (2005) Surf Sci 574:1